

# Real-Time In Vivo Assessment of Retinal Reattachment in Humans Using Swept-Source Optical Coherence Tomography



ADITYA BANSAL, WEI WEI LEE, TINA FEFELI, AND RAJEEV H. MUNI


- **PURPOSE:** To assess the in vivo physiology of retinal reattachment in humans using swept-source optical coherence tomography (SS-OCT) in real time.
- **DESIGN:** Prospective case series.
- **METHODS:** Fifteen consecutive patients with fovea-involving rhegmatogenous retinal detachment were undergoing pneumatic retinopexy. SS-OCT was performed at presentation and frequent intervals immediately after pneumatic retinopexy. The primary outcome was longitudinal assessment of early postoperative SS-OCT to establish stages of reattachment.
- **RESULTS:** Most patients (93.3%, 14/15) achieved successful reattachment at the median follow-up duration of 13 weeks (interquartile range 7.5-18.0). Reattachment occurred in 5 specific stages: 1) redistribution of fluid and approach of the neurosensory retina toward the retinal pigment epithelium occurred in 100% (15/15); 2) reduction in cystoid macular edema and improvement of outer retinal corrugations was achieved in 100% (15/15); 3) initial contact of the neurosensory retina to the retinal pigment epithelium occurred completely in 66.7% (10/15); 4) deturgescence of the inner and outer segments of the photoreceptors occurred in 66.7% (10/15); and 5) recovery of photoreceptor integrity occurred in 3 specific substages: 5A) external limiting membrane recovery (10/15, 66.6%); 5B) ellipsoid zone recovery (9/15, 60%); and 5C) interdigitation zone/foveal bulge recovery (3/15, 20%). Twenty percent (3/15) had delayed progression through stage 2, characterized by formation of outer retinal folds. Similarly, 33.3% (5/15) developed residual subfoveal fluid blebs (delayed progression to stage 3).

- **CONCLUSIONS:** This study characterizes the in vivo physiology of retinal reattachment in humans using high-resolution SS-OCT that occurs in 5 specific stages. Delayed progression through certain stages was characterized by postoperative anatomic abnormalities. *Am J Ophthalmol* 2021;221:•••–•••. © 2021 Elsevier Inc. All rights reserved. (*Am J Ophthalmol* 2021;227: 265–274. © 2021 Elsevier Inc. All rights reserved.)

Rhegmatogenous retinal detachment (RRD) is an acute sight-threatening emergency.<sup>1</sup> There have been numerous publications on the pathophysiology of RRD and the effectiveness of various techniques for surgical repair.<sup>2</sup> Despite substantial improvements in surgical techniques over the past century focused on increasing the single-operation reattachment rate, there is limited understanding regarding the comparative anatomic integrity of retinal reattachment with various techniques. The refinement of multimodal imaging has enhanced our ability to assess the integrity of postoperative anatomic outcomes. Many authors have evaluated a variety of optical coherence tomography (OCT) biomarkers after RRD repair and have assessed their association with functional outcomes.<sup>3–6</sup> For example, Kobayashi and associates<sup>7</sup> assessed photoreceptor microstructure using OCT and determined its association with postoperative visual acuity.

It has been demonstrated that pneumatic retinopexy (PnR) has a greater chance of achieving a high-integrity retinal attachment (HIRA) with less retinal displacement compared with pars plana vitrectomy (PPV).<sup>8</sup> Furthermore, PnR may be associated with better postoperative microstructural outer retinal integrity on OCT when compared with PPV.<sup>22</sup> These findings have led us to question how the retina is reattached with various techniques and if specific variations in surgical technique may lead to improvements in the integrity of anatomic attachment. There are also several postoperative anatomic complications after retinal detachment repair including persistent subretinal fluid, outer retinal folds, cystoid macular edema, and epiretinal membrane formation that may impact functional outcomes.<sup>9</sup> However, a detailed understanding of the pathophysiology of these complications is still evolving.

In 1968, Machemer<sup>10,11</sup> and Kroll and Machemer<sup>12,13</sup> conducted histologic and electron microscopy studies in

 Supplemental Material available at [AJO.com](https://www.ajocom.com).  
Accepted for publication February 12, 2021.

Department of Ophthalmology, St. Michael's Hospital/Unity Health Toronto, Toronto, Ontario, Canada; Department of Ophthalmology and Vision Sciences, University of Toronto, Toronto, Ontario, Canada; Dalla Lana School of Public Health, University of Toronto, Toronto, Ontario, Canada; Kensington Vision and Research Centre, University of Toronto, Toronto, Ontario, Canada; The Keenan Research Centre for Biomedical Science/Li Ka Shing Knowledge Institute, Toronto, Ontario, Canada

Inquiries to Rajeev H. Muni, Department of Ophthalmology, 8th floor, Donnelly Wing, St. Michael's Hospital, Unity Health Toronto, 30 Bond St, Toronto, Ontario, M5B 1W8, Canada.; e-mail: [rajeev.muni@gmail.com](mailto:rajeev.muni@gmail.com)

owl monkeys to assess changes that occur after surgically induced RRD and after retinal reattachment. Similarly, Lewis and associates<sup>14</sup> and Fisher and associates<sup>15</sup> used an experimental animal model of RRD to characterize cellular changes that occur after retinal detachment of varying durations and after reattachment.

There have been no human in vivo studies assessing the physiology of retinal reattachment. This is related to difficulty in assessing patients immediately postoperatively during the rapid reattachment that occurs in the first few hours after procedures such as PPV and scleral buckle. In PPV, the presence of a large gas bubble prevents detailed assessment of the retinal microstructure with OCT. With scleral buckle, significant postoperative swelling, ocular surface abnormalities, and patient discomfort limit proper early evaluation. The minimally invasive PnR, which uses a small expansile gas bubble that does not obstruct the visual axis and the availability of high resolution swept-source OCT (SS-OCT) provides a unique opportunity to assess the in vivo physiology of human retinal reattachment in a prospective longitudinal fashion in the first several hours and days after the intervention in real time.

---

## METHODS

- **STUDY DESIGN:** This was a prospective consecutive case series of patients with fovea-involving RRD undergoing PnR at St. Michael's Hospital/Unity Health Toronto, Toronto, Ontario, Canada between July 1, 2020 and September 30, 2020. This study was approved by the Research Ethics Board at St. Michael's Hospital/Unity Health Toronto in Toronto and adhered to the Declaration of Helsinki.

- **ELIGIBILITY:** Consecutive patients with a single or multiple retinal break(s) within 3 clock hours in detached retina above the 8- and 4-o'clock meridians with any number, location, and size of retinal breaks or lattice degeneration in the attached retina, proliferative vitreoretinopathy less than or equal to grade B, and who were undergoing treatment with PnR were eligible for the study. Exclusion criteria included a history of vitrectomy or scleral buckle in the affected eye, media opacity, and preexisting macular or retinal pathology.

- **PROCEDURE:** All patients underwent PnR as described in the PIVOT randomized trial.<sup>16</sup> Patients were given strict positioning instructions to place the apex of the bubble at the responsible retinal break(s), with or without the use of an initial steamroller maneuver with face-down positioning.

- **DATA COLLECTION AND IMAGING:** All patients had clinical examination and underwent imaging with the PLEX Elite 9000 SS-OCT using high-definition horizontal 1 line spotlight scan ( $\times 100$ ) and a 12-  $\times$  12-mm macular cube (Carl Zeiss, Dublin, California, USA). Imaging was performed at presentation and every 2 hours for the first 6 hours after gas injection, at days 1, 2, and 5, and at weeks 1, 2, 4, and 6 after PnR. Additional imaging was also performed at 3 months in most patients. Imaging of the detached retina was performed with the tracker off, with the aim of capturing a foveal scan. After retinal attachment, images were captured using FastTrac that mitigates eye motion and operator related artifacts to allow the same point to be compared over time.

- **OUTCOMES:** The primary outcome was the longitudinal assessment of the early postoperative SS-OCT changes after PnR for RRD to assess the in vivo human physiology of retinal reattachment in real time and to determine the stages of reattachment. All data are reported descriptively using medians and interquartile range (IQRs).

---

## RESULTS

Fifteen eyes of 15 consecutive patients with fovea involving RRD were enrolled. The demographic details and baseline clinical characteristics are shown in [Table 1](#). The median age at presentation was 62.0 years (IQR 55.0-72.5). The median number of days since loss of central vision was 14.0 days (IQR 7.5-27.0) and the median baseline logarithm of minimal angle of resolution (logMAR) visual acuity was 2.0 (Snellen equivalent: count fingers at 0.61 meters [IQR 1.5-2.7]).

One third (33.3%, 5/15) of patients presented within 3 days of central vision loss. The median clock hours of detachment was 8 (IQR 4.5-8.7). The median height of the retinal detachment at the fovea was 1006  $\mu$ m (IQR 899-1334  $\mu$ m). Almost all (93.3%, 14/15) patients had a successful retinal attachment with PnR at the median follow-up duration of 13.0 weeks (IQR 7.5-18.0 weeks). Median final logMAR visual acuity was 0.4 (Snellen equivalent 20/70 [IQR 0.1-0.6]).

All patients achieved retinal reattachment visible in real time on SS-OCT (Video 1; available online at [AJO.com](#)). Reattachment of every point on each patient's retina occurred in 5 specific stages ([Figure 1](#) and Data in Brief [Figures 1-4](#)). Although the stages of reattachment could be applied to any point on the retina, the emphasis for this study was on the fovea. Stage 1, defined as a redistribution of fluid and approach of the neurosensory retina towards the retinal pigment epithelium (RPE), occurred in 100% (15/15) of patients. Stage 1 had to demonstrate a

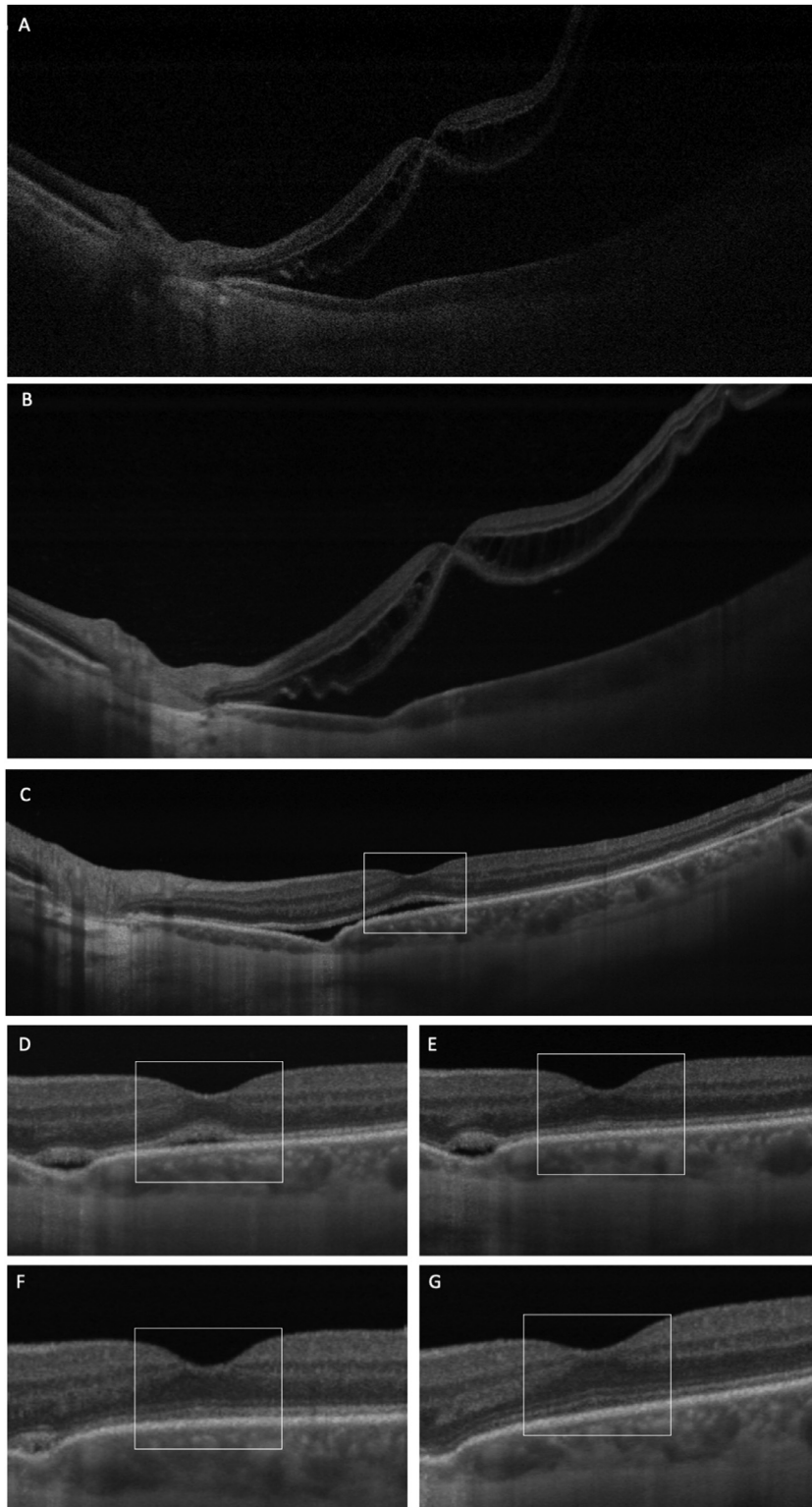


**FIGURE 1.** A. Baseline swept-source optical coherence tomography image showing rhegmatogenous retinal detachment with the presence of cystoid macular edema and outer retinal corrugations. B. Two hours after pneumatic retinopexy, the retina starts approaching the retinal pigment epithelium (stage 1). C and D. Six and 24 hours after pneumatic retinopexy, there is resolution of cystoid macular edema and outer retinal corrugations (stage 2). E. On day 2, there is contact between the retina and retinal pigment epithelium (stage 3) at the fovea (within the box). F. On day 3, there is deturgescence of the inner and outer segments of the photoreceptors (stage 4) at the fovea (within the box). G. At 6 weeks, there is a full recovery of photoreceptor integrity including the foveal bulge (stage 5C; within the box).

**TABLE 1. Baseline Demographic and Clinical Characteristics**

Patient No.	Age at Presentation (y)	Gender	No. of Days Since Loss of Central Vision	Lens Status	Laterality	Clock Hours of Detachment	Height of Detachment (Microns)	Baseline logMAR Visual Acuity
1	75	F	1	Phakic	OS	7	2897	1.3
2	58	M	2	Phakic	OS	8	903	1.3
3	76	F	19	Pseudophakic	OD	9	1006	1.3
4	69	F	21	Phakic	OD	6	1062	1.3
5	23	F	14	Phakic	OS	4	81	0.3
6	62	M	2	Pseudophakic	OS	9	1463	3.0
7	52	M	14	Phakic	OS	12	895	1.3
8	52	M	0	Pseudophakic	OD	8	32	0.4
9	71	M	11	Phakic	OS	8	2110	1.4
10	57	M	10	Pseudophakic	OD	9	592	0.7
11	56	M	1	Phakic	OS	4	942	0.7
12	54	M	14	Phakic	OS	3	1283	2.0
13	77	M	15	Phakic	OD	8	1385	3.0
14	73	M	40	Phakic	OD	4	1136	2.0
15	72	M	27	Phakic	OD	8	911	1.0

F = female; logMAR = logarithm of minimal angle of resolution; M = male; OD = right eye; OS = left eye.

reduction in the height of the RRD compared with baseline. Stage 2 is characterized by a reduction in cystoid macular edema (CME) and improvement of outer retinal corrugations which was also achieved in 100% (15/15) of patients. Stage 3 is defined by the initial contact of the neurosensory retina to the RPE which occurred completely in 66.7% (10/15) and incompletely in 33.3% (5/15) of patients. Stage 4 was defined as deturgescence of the inner and outer segments of the photoreceptors which occurred completely in 66.7% (10/15) of patients. Stage 5 was characterized by a recovery of photoreceptor integrity which occurred in 3 substages (5A, external limiting membrane [ELM; 10/15, 66.7%]; 5B, ellipsoid zone [EZ; 9/15, 60%]; and 5C, interdigitation zone/foveal bulge [3/15, 20%; Table 2]).

Twenty percent (3/15) of patients failed to have complete resolution of outer retinal corrugations in stage 2 which led to the formation of outer retinal folds when parts of the retina adjacent to the persistent outer retinal corrugations properly reattached. The outer retinal folds gradually resolved in all cases over several weeks and the involved parts of the retina subsequently progressed to stage 3 and beyond (Figure 2). Similarly, 33.3% (5/15) of patients failed to have complete resolution of subfoveal fluid with specific areas of noncontact of the neurosensory retina to the RPE with the formation of residual subfoveal fluid blebs and delayed progression to stage 3 (Figure 3). These blebs were responsible for those cases above that had incomplete passage through stages 3 and 4. It is only after the slow reabsorption of the subfoveal fluid that there can be progression to stage 3 and

beyond. Eighty percent (4/5) of cases with subfoveal fluid blebs were noted in patients >65 years of age with delayed presentation (>3 days) and a baseline height of detachment at the fovea of  $\geq 1000 \mu\text{m}$ .

When assessing patients with acute ( $\leq 3$  days) or delayed progression (>3 days) there were no substantial differences in the progression through the stages of reattachment and both groups followed the same consistent sequence. However, at the 3-month time point, 40% (2/5) of patients in the acute presentation group vs 10% (1/10) in the delayed presentation group achieved stage 5C. In addition, 42.9% (3/7) of patients with height of detachment  $<1000 \mu\text{m}$  achieved stage 5C at 3 months, whereas none of the eyes with height  $\geq 1000 \mu\text{m}$  (n = 8) achieved stage 5C.

Median logMAR visual acuity at 72 hours after PnR was 0.7 (Snellen equivalent: 20/100 [IQR 0.5-1.0]) with the median stage of reattachment being stage 4. By 2 weeks, median logMAR visual acuity and median stage of reattachment improved to 0.6 (Snellen equivalent: 20/80 [IQR 0.4-1.0]) and stage 5A, respectively. At both 4-6 weeks and 3 months, median logMAR visual acuity and stage of retinal attachment were 0.5 (Snellen equivalent: 20/60 [IQR 0.2-0.5 for 4-6 weeks, IQR 0.1-0.7 for 3 months]) and stage 5B, respectively.

• **DISCUSSION:** We assessed the in vivo human physiology of retinal reattachment for the first time. PnR provides an ideal model to study retinal reattachment and the availability of high-definition SS-OCT allows for high-resolution imaging in real time. This unique combination allowed for

**TABLE 2.** Stages of Retinal Reattachment and Postoperative Anatomic Abnormalities at Various Time Points

Patient No.	Retinal Attachment Stage						
	1	2	3	4	5A	5B	5C
1	2 hrs	6-24 hrs	Bleb	—	—	—	—
2	2 hrs	6 hrs	48 hrs	72 hrs	Intact	Intact	6 wks
3	2 hrs	6 hrs	Bleb	—	—	—	—
4	2 hrs	6 hrs	6 hrs	24 hrs	2-3 wks	6 wks	—
5	2 hrs	6-24 hrs	Bleb	—	—	—	—
6	2 hrs	4 hrs	24 hrs	72 hrs	1-2 wks	6 wks	—
7	2 hrs	2 hrs	4 hrs	6-24 hrs	2-4 wks	6 wks	—
8	2 hrs	2 hrs	4 hrs	24 hrs	Intact	Intact	2-6 wks
9 <sup>a</sup>	2 hrs	6-24 hrs	Bleb	—	—	—	—
10	2 hrs	6-24 hrs	48 hrs	48 hrs	Intact	2 wks	6 wks
11 <sup>b</sup>	2 hrs	6-24 hrs	24 hrs	24 hrs	4-6 wks	—	—
12 <sup>b</sup>	2 hrs	6-24 hrs	24 hrs	24 hrs	Intact	6-12 wks	—
13	2 hrs	6-24 hrs	Bleb	—	—	—	—
14 <sup>b</sup>	2 hrs	6-24 hrs	24 hrs	48 hrs	2 wks	4-6 wks	—
15	2 hrs	4 hrs	6 hrs	24 hrs	4-6 wks	6-12 wks	—

<sup>a</sup>Recurrence of rhegmatogenous retinal detachment at 3 months.

<sup>b</sup>Outer retinal folds resolved.

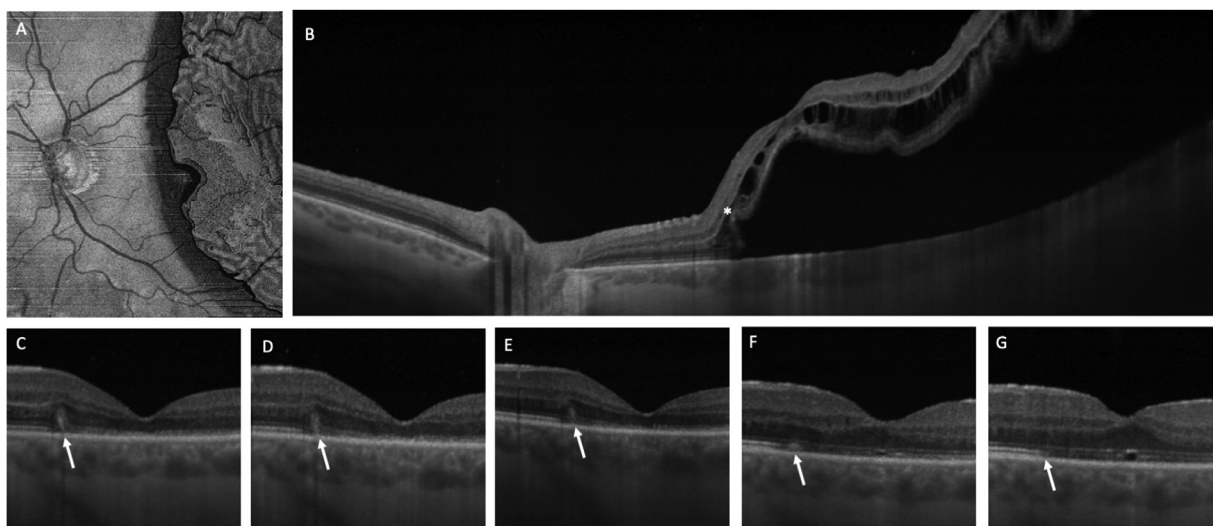


**FIGURE 2.** A and B. Infrared fundus image and baseline swept-source optical coherence tomography image demonstrating the extent of rhegmatogenous retinal detachment, along with the presence of cystoid macular edema and outer retinal corrugations (asterisk). C. Twenty-four hours after pneumatic retinopexy, there is a contact of the retina with retinal pigment epithelium before resolution of outer retinal corrugations leading to the formation of an outer retinal fold (stage 2; arrow). D and E. Resolving outer retinal fold by 3-4 weeks after pneumatic retinopexy (stage 2). F. On day 28, contact occurs between the retina and the retinal pigment epithelium (stage 3) at the location of the previous fold (arrow). G. At 6 weeks, there is deturgescence of inner and outer segments of photoreceptors (stage 4) at the location of the previous fold (arrow).



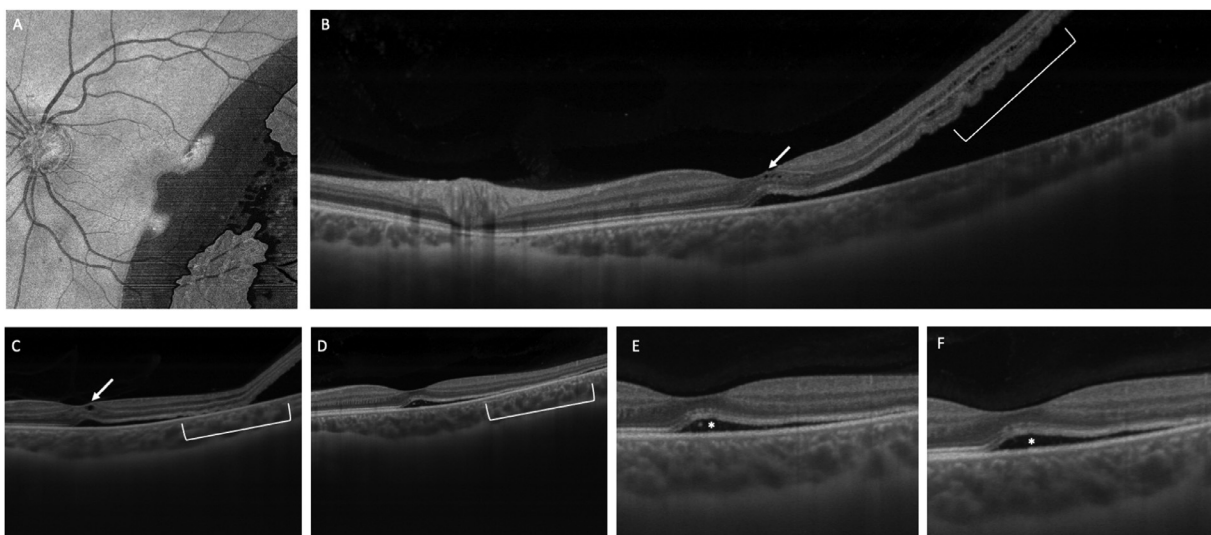


**FIGURE 3.** A and B. Infrared fundus image and baseline swept-source optical coherence tomography image demonstrating the extent of rhegmatogenous retinal detachment, along with the presence of cystoid macular edema (arrow) and outer retinal corrugations (bracket). C. Four hours after pneumatic retinopexy, the retina starts approaching the retinal pigment epithelium (stage 1). D. Twenty-four hours after pneumatic retinopexy, there is the improvement of cystoid macular edema and outer retinal corrugations (stage 2; bracket). E and F. At weeks 1 and 6 after pneumatic retinopexy, there is a persistent subretinal fluid bleb (asterisk) in the subfoveal and surrounding area leading to a delayed progression to stage 3.

the development of a novel staging system that describes the physiology of retinal reattachment. In addition, we were able to determine that when there was a delay in completing a specific stage, which was characterized by predictable anatomic abnormalities, such as outer retinal folds or persistent subretinal fluid blebs, there still appeared to be a progression through the remaining stages in a consistent and predictable succession (Figures 2 and 3).

In 1968, Machemer<sup>10,11</sup> and Kroll and Machemer<sup>12,13</sup> undertook the difficult task of understanding the histologic changes and electron microscopy features of an experimentally detached retina in owl monkeys. In the early stages of detachment, they found cystoid edema in the inner retina, which progressed to involve the outer layers. The histologic changes at baseline observed by Machemer<sup>10</sup> are consistent with the CME and outer retinal corrugations that are typically observed at baseline on optical coherence tomography.<sup>3,17</sup> In further experiments, after reattaching the retina, Machemer<sup>11</sup> demonstrated that although the retina was grossly attached, the outer retinal layers still appeared wavy and irregular, which may be consistent with persistent outer retinal folds and subretinal blebs as seen in this study.

There were several insights gained from Machemer's early histologic studies<sup>10,11</sup> that can now be more thoroughly understood in the context of the staging system for

retinal reattachment described in this study. First, he suggested that there was an altered metabolism of the RPE that was overwhelmed from the large amount of subretinal fluid, and this resulted in the intraretinal edema on histologic sections. We observed a rapid improvement in the CME in stage 2 even before contact of the retina with the RPE. This is likely occurring because of improved metabolic transfer between the retina and the RPE and the removal of intraretinal fluid by the RPE pump as the height of the detachment is rapidly reduced (stage 1). Machemer<sup>10</sup> also hypothesized that the intraretinal edema involving the outer retina resulted in folds in the detached retina, which is consistent with the outer retinal corrugations seen in most patients at baseline. More recently, Dalvin and associates<sup>18</sup> have proposed that under the circumstances of altered subretinal fluid composition and an overwhelmed RPE pump, glycosaminoglycans in the interphotoreceptor matrix become hydrated, resulting in swelling and expansion of the photoreceptor outer segments, resulting in hydration folds, seen as outer retinal corrugations on OCT. However, animal histologic studies have shown degeneration of the photoreceptor outer segments soon after induced retinal detachment,<sup>10,14</sup> and Hollyfield and associates<sup>19</sup> also demonstrated that the interphotoreceptor matrix surrounds both the inner and outer segments. Therefore, we believe that hydration is occurring in both the remain-

ing outer segments as proposed by Dalvin and associates<sup>18</sup> but also in the region of the inner segments, particularly the EZ.

Lewis and associates<sup>14</sup> found that retinal detachment does not result in complete cellular destruction but is rather limited to photoreceptor degeneration. They found that photoreceptors and RPE apical microvilli degenerate even after short periods of detachment and outer segment lengths reduce progressively with duration of retinal detachment. After retinal reattachment, they found that the RPE/photoreceptor interface does not recover fully even after an extended period of time and that the extent of outer segment regrowth and alignment varies over long stretches of reattachment.<sup>14,15</sup> These findings are consistent with the marked early abnormalities in the outer retinal microstructure that slowly recovered over time in this study.

This in vivo real-time assessment of retinal reattachment demonstrated that the retina reattaches in 5 specific and predictable stages (Figure 4 and Video 2). The injection of intravitreal gas occluded the retinal break and led to a cessation of liquefied vitreous entering the subretinal space. This led to stage 1, characterized by a rapid reduction in the height of the detachment and an approach of the retina to the RPE. This reduction in height of the detachment likely resulted in improved metabolic transport between the retina and the RPE, resulting in a dehydration of the inner and outer retina, with reduction of CME and improvement in hydration folds/outer retinal corrugations, which defines stage 2. It is important to note that the reduction of CME and improvement in outer retinal corrugations generally starts occurring before the initial contact of the retina with the RPE when the retina reattaches in a natural manner with PnR. Once the retina has made contact with the RPE, stage 3 has been achieved. This is followed by a rapid deturgescence of the inner and outer segments of the photoreceptors that characterizes stage 4. Stage 5 is characterized by an improvement in the integrity of the outer retina which occurred in sequence from the external limiting membrane, to the EZ, to the interdigitation zone, and/or recovery of the foveal bulge. Consistent with our findings, Wakabayashi and associates<sup>4</sup> also demonstrated that the integrity of the ELM was a prerequisite to EZ recovery. In terms of the timing to achieve stage 5, we noted that this was dependent on chronicity. Both Machemer et al<sup>10</sup> and Lewis and associates<sup>14</sup> also found that the duration of detachment was related to the degeneration and apoptosis of photoreceptors. Therefore, in some cases of acute RRD, where we have clear documentation of the patient having central vision loss for <48 hours (Figure 1), the outer retinal integrity may still be intact. In this case, as the patient achieved reattachment with completion of stage 4 (inner and outer segment deturgescence), stages 5A and 5B were skipped because the

ELM and EZ were already intact and the patient then progressed to stage 5C.

The final stage (5C), recovery of the foveal bulge, was achieved in 3 patients in our cohort. These results are consistent with studies by Dell'Omo and associates<sup>20</sup> and Kobayashi and associates,<sup>7</sup> who found that it took an extended period of time for recovery of the foveal bulge in macula-off RRD. In our study, most patients achieved a substantial improvement in the integrity of the ELM and EZ at 6 weeks.

An understanding of the stages of retinal reattachment provides several important benefits. First, it enhances our understanding of certain anatomic abnormalities that occur after retinal reattachment. Twenty percent of patients in our cohort developed outer retinal folds. It was evident that this occurred because certain points on the retina remained in stage 2, despite adjacent areas progressing to stage 3. This led to persisting outer retinal corrugations developing into outer retinal folds. After several weeks, the folds resolved with progression to stage 3 and beyond (Figure 2). Outer retinal folds are a well characterized anatomic abnormality that occur after RRD repair, particularly with PPV as described by Dell'omo and associates,<sup>21</sup> but can also occur after PnR. Another abnormality that was observed was delayed progression beyond stage 2, characterized by the incomplete reabsorption of subretinal fluid and the development of residual subfoveal fluid blebs in 33.3% of patients. However, it was noted that as the residual subfoveal fluid blebs resolved, patients progressed to stage 3 and beyond in predictable sequence.

This study has several strengths. This was a prospective study, with frequent imaging using SS-OCT after gas bubble injection, which allowed us to observe retinal reattachment in real time. This study was performed in patients undergoing PnR, where a small expansile bubble occludes the retinal break, and the subretinal fluid is reabsorbed naturally by the RPE pump. This is the ideal model in which to assess the human physiology of retinal reattachment in response to PnR and likely other techniques of retinal reattachment that are dependent on the action of the RPE pump.

There are certain limitations of this study. The sample size of 15 is relatively small and future studies with more patients would be worthwhile. However, we noticed consistency in the stages of reattachment in the 15 patients we followed and the frequent imaging over a long section of the central retina (12-16 mm) with SS-OCT allowed us to assess the stages of reattachment at several points on each retina. The follow-up was relatively short because the purpose was to observe the acute phases of reattachment in real time. Studies with longer follow-up will be useful to further assess the timing of stages 5A to 5C in greater detail.

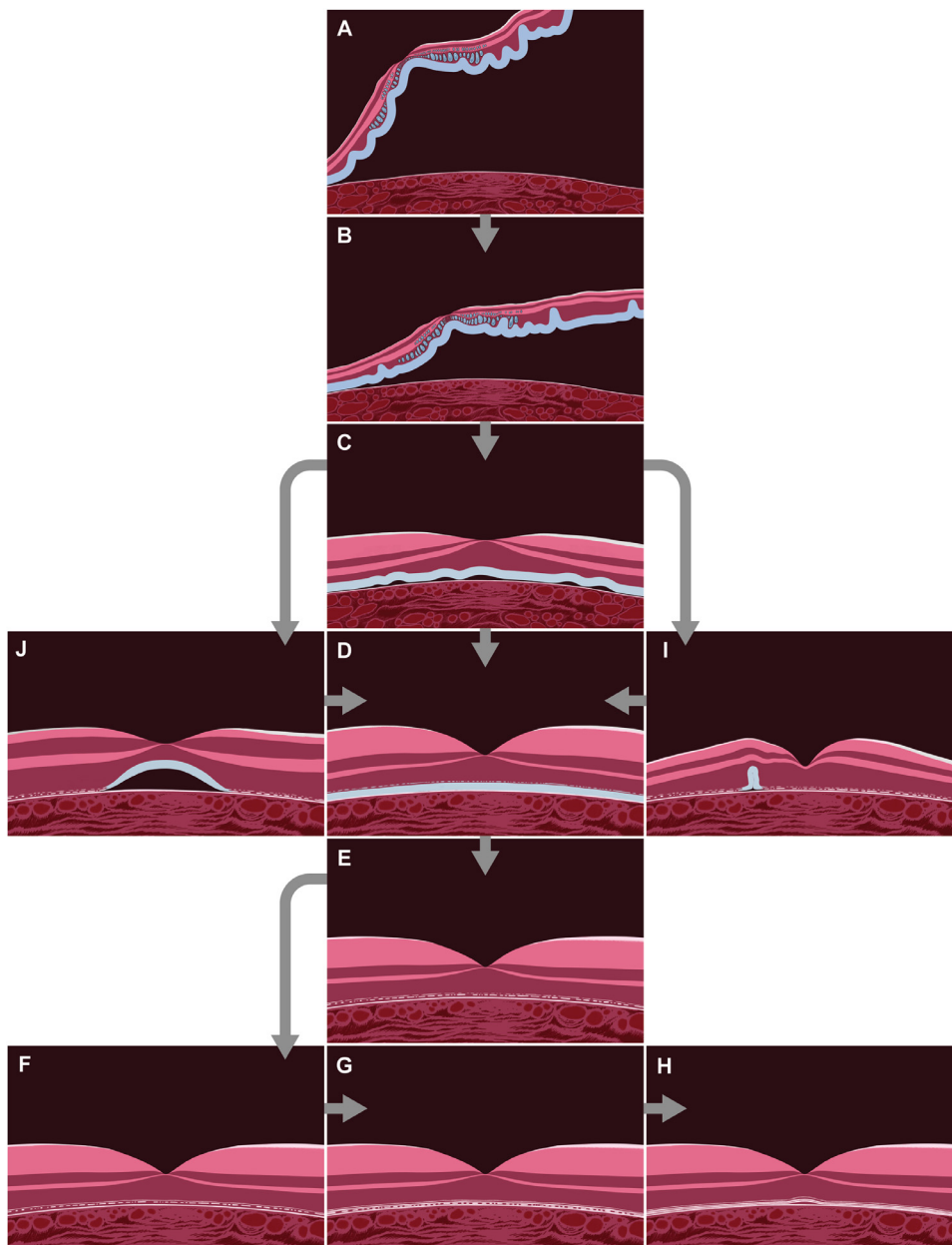


**FIGURE 4.** Illustration demonstrating the stages of retinal reattachment. A. Baseline status demonstrating a detached retina with cystoid macular edema and outer retinal corrugations. B. Stage 1: reduction in the height of the retinal detachment. C. Stage 2: significant improvement in cystoid macular edema and outer retinal corrugations. D. Stage 3: initial contact of the neurosensory retina to the retinal pigment epithelium. E. Stage 4: deturgescence of the photoreceptor inner and outer segments. F. Recovery of photoreceptor integrity, stage 5A: recovery of the external limiting membrane integrity. G. Stage 5B: recovery of the ellipsoid zone integrity. H. Stage 5C: recovery of the interdigitation zone and foveal bulge integrity. I. Demonstrating incomplete resolution of an outer retinal corrugation when the surrounding retina has progressed through stage 3 or beyond, which leads to the formation of an outer retinal fold (delayed progression through stage 2) at the same location. The outer fold eventually resolves leading to stage 3 and beyond at that specific point on the retina. J. Demonstrating residual subretinal fluid bleb (delayed progression to stage 3). After the slow reabsorption of the subretinal fluid and contact of the neurosensory retina with the retinal pigment epithelium (stage 3), there is progression to stage 4 and beyond at that specific point on the retina. A high-resolution version of the images are available online as eSlide: VM01.



In conclusion, this study has assessed the physiology of retinal reattachment in real time using SS-OCT. We have found that retinal reattachment occurs in specific stages and that delayed progression through certain stages was characterized by anatomic abnormalities, such as outer retinal folds and residual subfoveal fluid blebs. Future studies will

focus on how various surgical techniques modify the physiology of retinal reattachment and will allow vitreoretinal surgeons to optimize surgical procedures to maximize the integrity of attachment and functional outcomes after retinal detachment repair.

All authors have completed and submitted the ICMJE form for disclosure of potential conflicts of interest. Funding/Support: This study received no funding. Financial Disclosures: The authors indicate no financial support or conflicts of interest. All authors attest that they meet the current ICMJE criteria for authorship.

This study was approved by the Research Ethics Board at St Michael's Hospital/Unity Health Toronto, Toronto, Ontario, Canada, and adhered to the Declaration of Helsinki. All human subjects were recruited after written informed consent. Aditya Bansal was responsible for the methodology, data curation, investigation, and writing the original draft. Wei Wei Lee was responsible for the conceptualization, methodology, and resources. Tina Felfeli was responsible for the methodology, data curation, and resources. Rajeev H. Muni was responsible for the conceptualization, methodology, writing the original draft, reviewing and editing, and supervision.

## REFERENCES

1. Mitry D, Chalmers J, Anderson K, et al. Temporal trends in retinal detachment incidence in Scotland between 1987 and 2006. *Br J Ophthalmol*. 2011;95(3):365–369.
2. Saw SM, Gazzard G, Wagle AM, et al. An evidence-based analysis of surgical interventions for uncomplicated rhegmatogenous retinal detachment. *Acta Ophthalmol Scand*. 2006;84(5):606–612.
3. Hagimura N, Suto K, Iida T, Kishi S. Optical coherence tomography of the neurosensory retina in rhegmatogenous retinal detachment. *Am J Ophthalmol*. 2000;129(2):186–190.
4. Wakabayashi T, Oshima Y, Fujimoto H, et al. Foveal microstructure and visual acuity after retinal detachment repair. Imaging analysis by Fourier-domain optical coherence tomography. *Ophthalmology*. 2009;116(3):519–528.
5. Hasegawa T, Ueda T, Okamoto M, Ogata N. Relationship between presence of foveal bulge in optical coherence tomographic images and visual acuity after rhegmatogenous retinal detachment repair. *Retina*. 2014;34(9):1848–1853.
6. Noda H, Kimura S, Morizane Y, et al. Relationship between preoperative foveal microstructure and visual acuity in macula-off rhegmatogenous retinal detachment: imaging analysis by swept source optical coherence tomography. *Retina*. 2020;40(10):1873–1880.
7. Kobayashi M, Iwase T, Yamamoto K, et al. Association between photoreceptor regeneration and visual acuity following surgery for rhegmatogenous retinal detachment. *Investig Ophthalmol Vis Sci*. 2016;57(3):889–898.
8. Brosh K, Francisconi CLM, Qian J, et al. Retinal displacement following pneumatic retinopexy vs pars plana vitrectomy for rhegmatogenous retinal detachment. *JAMA Ophthalmol*. 2020;138(6):652–659.
9. Lv Z, Li Y, Wu Y, Qu Y. Surgical complications of primary rhegmatogenous retinal detachment: a meta-analysis. *PLoS One*. 2015;10(3):1–13.
10. Machemer R. Experimental retinal detachment in the owl monkey. II. Histology of retina and pigment epithelium. *Am J Ophthalmol*. 1968;66(3):396–410.
11. Machemer R. Experimental retinal detachment in the owl monkey. IV. The reattached retina. *Am J Ophthalmol*. 1968;66(6):1075–1091.
12. Kroll AJ, Machemer R. Experimental retinal detachment in the owl monkey. III. Electron microscopy of retina and pigment epithelium. *Am J Ophthalmol*. 1968;66(3):410–427.
13. Kroll AJ, Machemer R. Experimental retinal detachment in the owl monkey. V. Electron microscopy of the reattached retina. *Am J Ophthalmol*. 1969;67(1):117–130.
14. Lewis GP, Charteris DG, Sethi CS, Fisher SK. Animal models of retinal detachment and reattachment: identifying cellular events that may affect visual recovery. *Eye*. 2002;16(4):375–387.
15. Fisher SK, Lewis GP, Linberg KA, Verardo MR. Cellular remodeling in mammalian retina: results from studies of experimental retinal detachment. *Prog Retin Eye Res*. 2005;24(3):395–431.
16. Hillier RJ, Felfeli T, Berger AR, et al. The pneumatic retinopexy versus vitrectomy for the management of primary rhegmatogenous retinal detachment outcomes randomized trial (PIVOT). *Ophthalmology*. 2019;126(4):531–539.
17. Lee SY, Joe SG, Kim JG, et al. Optical coherence tomography evaluation of detached macula from rhegmatogenous retinal detachment and central serous chorioretinopathy. *Am J Ophthalmol*. 2008;145(6):1071–1076.
18. Dalvin LA, Spaide RF, Yannuzzi LA, et al. Hydration folds in rhegmatogenous retinal detachment. *Retin Cases Brief Rep*. 2020;14(4):355–359.
19. Hollyfield JG. Hyaluronan and the functional organization of the interphotoreceptor matrix. *Investig Ophthalmol Vis Sci*. 1999;40(12):2767–2769.

20. Dell'Omo R, Viggiano D, Giorgio D, et al. Restoration of foveal thickness and architecture after macula-off retinal detachment repair. *Investig Ophthalmol Vis Sci*. 2015;56(2):1040–1050.
21. Dell'Omo R, Stevie Tan H, Schlingemann RO, et al. Evolution of outer retinal folds occurring after vitrectomy for retinal detachment repair. *Investig Ophthalmol Vis Sci*. 2012;53(13):7928–7935.
22. Muni Rajeev H, Felfeli Tina, Sadda Srinivas R, et al. Postoperative Photoreceptor Integrity Following Pneumatic Retinopathy vs Pars Plana Vitrectomy for Retinal Detachment Repair: A Post Hoc Optical Coherence Tomography Analysis From the Pneumatic Retinopexy Versus Vitrectomy for the Management of Primary Rhegmatogenous Retinal Detachment Outcomes Randomized Trial.. *JAMA ophthalmology*. 2021 In press. doi:[10.1001/jamaophthalmol.2021.0803](https://doi.org/10.1001/jamaophthalmol.2021.0803).